Coronal Heating and Cooling, and its Imprints on the Rapid Aperiodic Variability of X-ray Binaries

M. Böttcher

(Chandra Fellow)

Physics and Astronomy Dept., Rice University, Houston, TX, USA

Abstract

The most popular models for the complex phase and time lags in the rapid aperiodic variability of Galactic X-ray binaries are based Comptonization of soft seed photons in a hot corona, where small-scale flares are induced by flares of the soft seed photon input (presumably from a cold accretion disc). However, in their original version, these models have neglected the additional cooling of the coronal plasma due to the increased soft seed photon input, and assumed a static coronal temperature structure. In this paper, our Monte-Carlo/Fokker-Planck code for time-dependent radiation transfer and electron energetics is used to simulate the self-consistent coronal response to the various flaring scenarios that have been suggested to explain phase and time lags observed in some Galactic X-ray binaries. It is found that the predictions of models involving slab-coronal geometries are drastically different from those deduced under the assumption of a static corona. However, with the inclusion of coronal cooling they may even be more successful than in their original version in explaining some of the observed phase and time lag features. The predictions of the model of inward-drifting density perturbations in an ADAF-like, two-temperature flow also differ from the static-corona case previously investigated, but may be consistent with the alternating phase lags seen in GRS 1915+105 and XTE J1550-564. Models based on flares of a cool disc around a hot, inner two-temperature flow may be ruled out for most objects where significant Fourier-frequency-dependent phase and time lags have been observed.

Baltimore, MD, April 4 – 6, 2001

1) Different model setups and the numerical method

Geometrical scenarios:

a) A slab geometry with a cool, optically thick accretion disk (Shakura & Sunyaev 1973) sandwiched by a hot, tenuous corona (Liang & Price 1977, Bisnovatyi-Kogan & Blinnikov 1977); rapid variability is caused by flares in the underlying accretion disk (see Section 2)

b) A two-phase accretion disk with transition from an inner, hot coronal flow (possibly ADAF [Narayan & Yi 1994, Chen et al. 1995], CDAF [Quataert & Gruzinov 2000], or ADIOS [Blandford & Begelman 1999]) to an outer, cool, Shakura-Sunyaev-type accretion disk (Narayan, McClintock & Yi 1996, Esin et al. 1998); rapid variability is caused by flares in the outer, cool disk (see Section 3)

c) Blobs or rings of cool material drifting inward through an inner, hot coronal flow (ADAF, CDAF, ADIOS) from the radius of transition to an outer, cool Syakura-Sunyaev-type accretion disk (Böttcher & Liang 1999) (see Section 4)

Numerical procedure:

The coupled Monte-Carlo / Fokker-Planck code developed in Böttcher & Liang (2001) is used. It includes the following processes self-consistently in a time- and space-dependent simulation:

- Compton scattering
- Cyclotron / synchrotron emission and absorption
- Bremsstrahlung emission and absorption
- Coulomb heating of electrons by a background pool of hot ions
- Nonthermal electron acceleration via Alfvén/whistler wave turbulence
- Radiative cooling of electrons due to all of the above radiation mechanisms

2) The slab-corona case

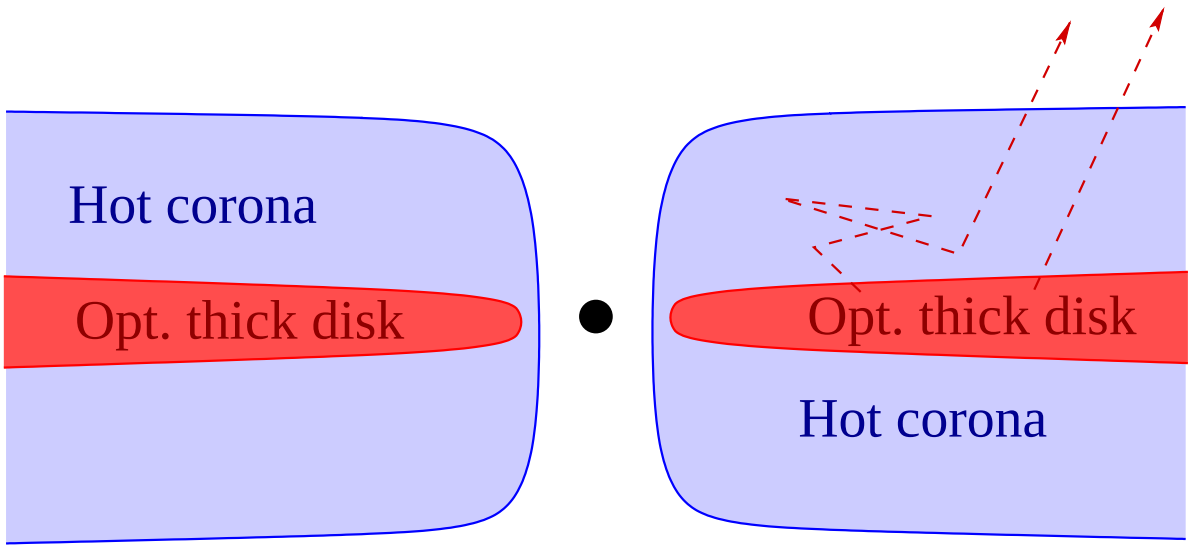

- Shakura-Sunyaev disk sandwiched by hot corona
- "quiescent" disk temperature: $kT_{D,qu} = 0.2$ keV
- Disk temperature during flares: $kT_{D,fl} = 0.5$ keV
- Proton temperature in crona: $kT_p = 100$ MeV
- Thomson depth of corona: $\tau_T = 1$
- Height of corona: $h = 10^8$ cm

Investigate the effect of accretion-disk flares
of different duration $\Delta t_{\rm flare}$

Light curves:

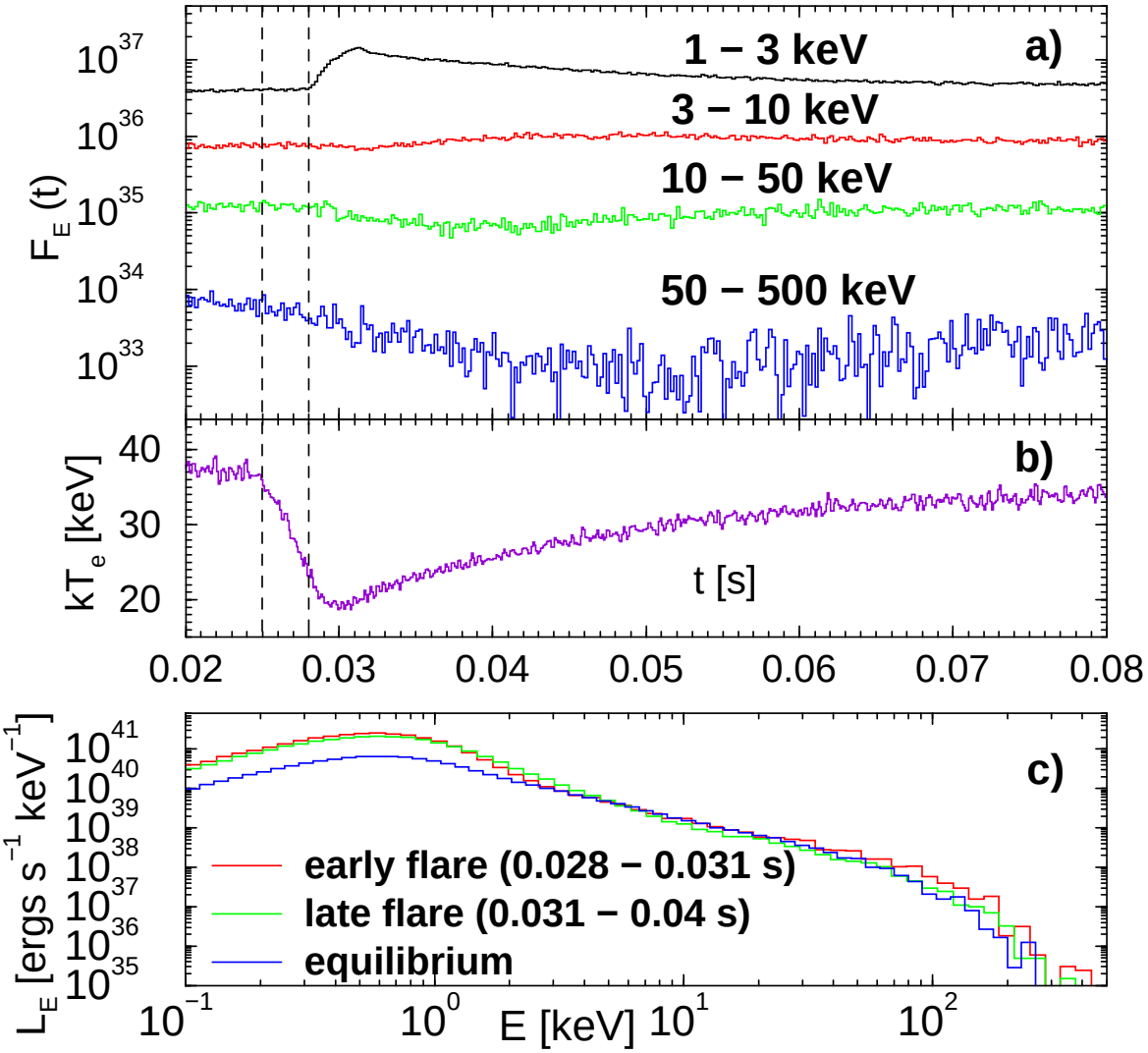

Fig. 2: *Energy-dependent light curves (a), evolution of the average coronal temperature (b), and snap-shot spectra (c) resulting from an accretion-disk flare in slab-coronal geometry lasting* $\Delta t_{\rm flare} = 3 \times 10^{-3}$ *s, during which the accretion-disk temperature is increased from 0.2 to 0.5 keV.*

Phase and time lags:

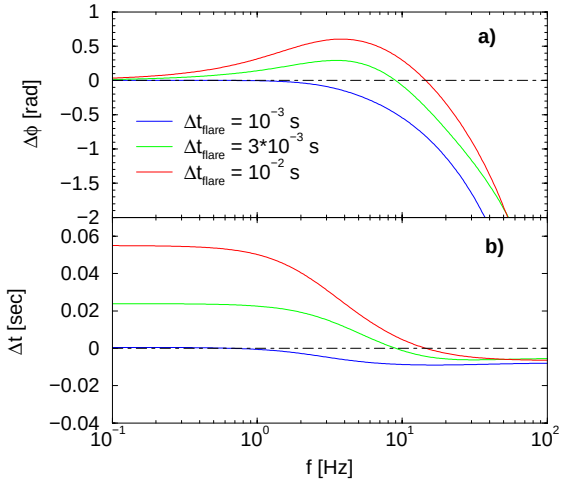

Fig. 3: *Phase (a) and time (b) lags from accretion-disk flares in slab-coronal geometry assuming different durations* $\Delta t_{\rm flare}$ *of the accretion disk flare.*

Energy-dependence of time lags

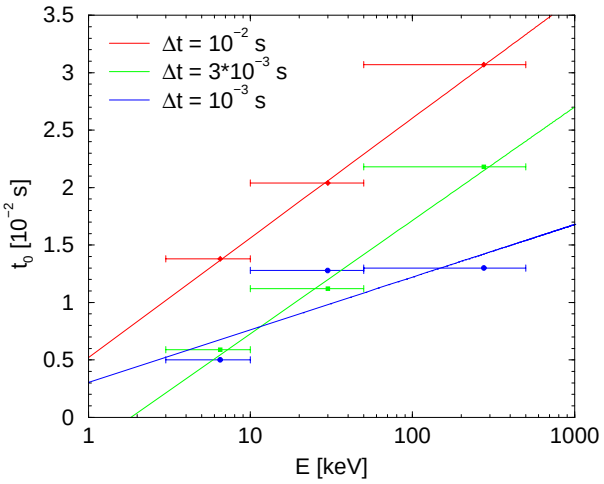

Fig. 4: *Light curve parameter* t_0*, determining the maximum time lag from an accretion-disk flare scenario in slab-coronal geometry assuming different durations* $\Delta t_{\rm flare}$ *of the accretion disk flare.*

Results for slab-corona case:

- Light curves look drastically different than under the assumption of a static (constant-temerature) corona, as used in earlier papers (Kazanas et al. 1997, Hua et al. 1997, Böttcher & Liang 1998)

- Pivoting of X-ray spectra around $\sim$ 20 keV rather than high-energy flares (see also Malzac & Jourdain 2000)

- When interpreting recovery phase as "onset of flare": No significant peak misalignment between flares at high and low photon energies, as generally observed (Paul et al. 1998a,b, Maccarone et al. 2000)

- Linear time-lag vs. Fourier period relation over limited frequency range, as observed in many X-ray binaries

- Negative phase lags possible

- Time lag vs. photon energy: $\Delta t_{\rm max} \propto \ln(E)$, in agreement with observations

- Time lags determined by Coulomb heating time scale,

$$\tau_{\rm Coulomb} \sim 3 \times 10^{-3}\, n_{15}^{-1}\, \frac{\Theta_e}{\Theta_p}\, (\Theta_e + \Theta_p)^{3/2}\ {\rm s}$$

  independent of the size of the corona. This solves the problem of large coronal sizes required in the framework of static-corona calculations

3) The outer-cool-disk case

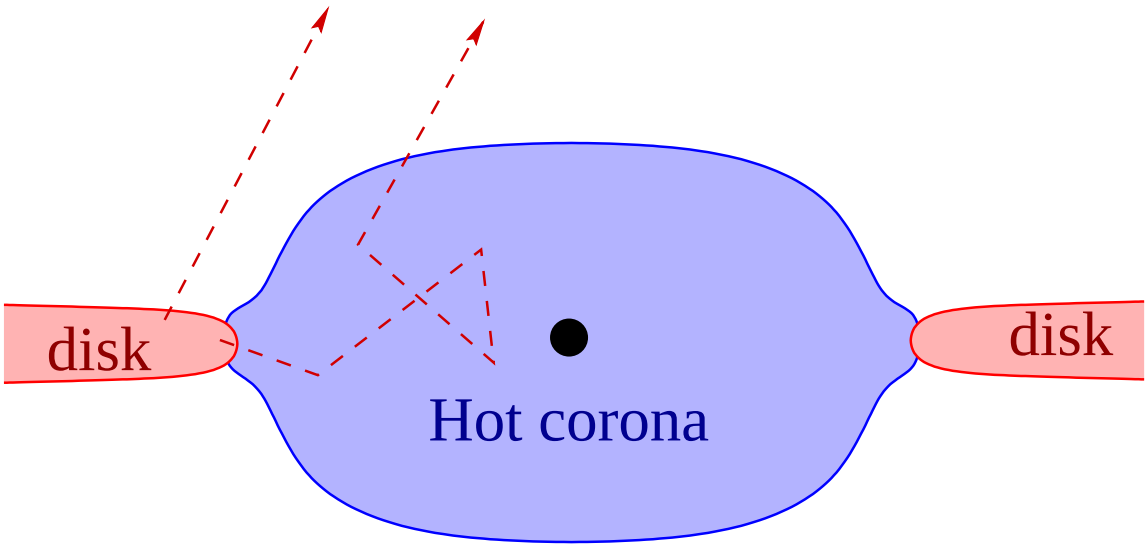

- Inner, hot accretion flow (ADAF; results are insensitive to details of the coronal flow), transition to outer, Shakura-Sunyaev-type flow at $r_{\rm tr}$
- Parameters typical for those deduced for GRS 1915+105: $r_{\rm tr} = 60$ km; $\tau_{\rm T}^{\rm corona} = 0.75$, $kT_{\rm BB} = 1$ keV
- During accretion-disk flare: $kT_{\rm BB} \rightarrow 2$ keV

Investigate the effect of accretion-disk flares
of different duration $\Delta t_{\rm flare}$

Energy-dependent light curves:

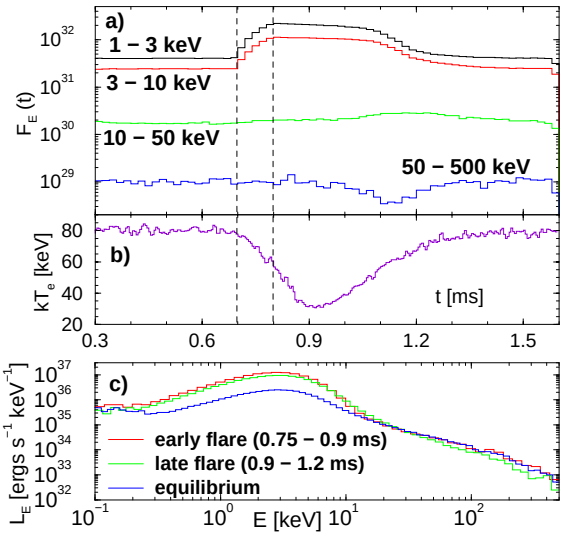

Fig. 6: *Energy-dependent light curves (a), average coronal temperature (b), and snap-shot spectra from accretion-disk flares in outer-cool-disk / inner-corona geometry assuming a flare time scale* $\Delta t_{\rm flare} = 10^{-4}$ *s.*

Results for outer-disk case

- Pivoting of spectrum rather than high-energy flare
- Very short coronal response time scales $\Longrightarrow$ requires extreme conditions (e.g., very low densities) to produce time lags $\gtrsim 1$ ms
- Significant peak misalignment between different energy channels, in contrast to observations

$\Longrightarrow$ **This scenario may be ruled out**
(at least for objects in which
significant time lags have been found)

4) The inward-drifting-blob case

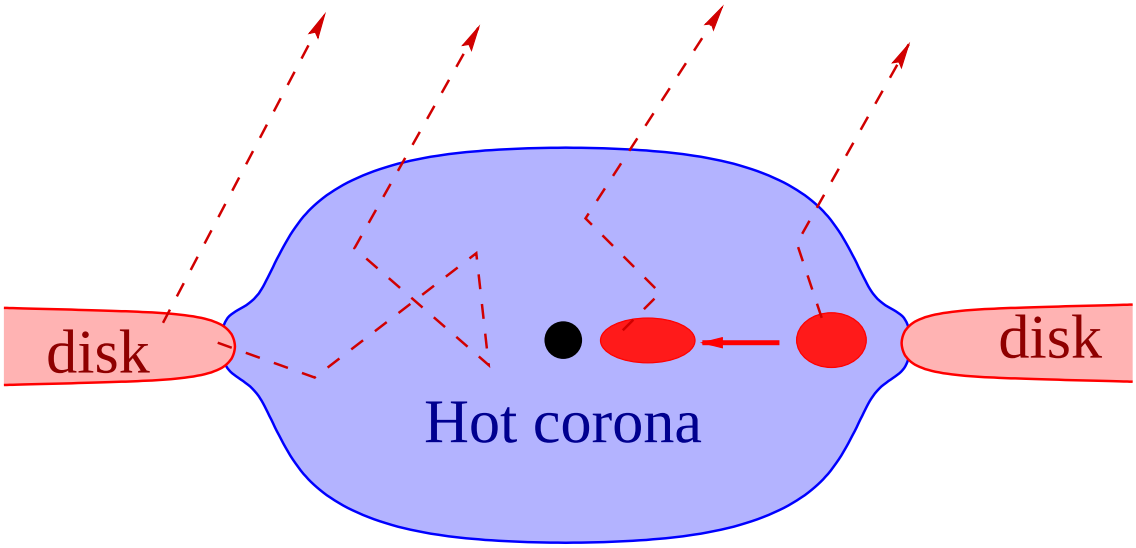

- Same corona/disk setup as in previous case: coronal ADAF and outer Shakura-Sunyaev disk with $r_{\rm tr} = 60$ km; $\tau_{\rm T}^{\rm corona} = 0.75$, $kT_{\rm BB} = 1$ keV
- Blobs (or rings) of cool material drifting inward from $r_{\rm tr}$ towards the event horizon, radial velocity $\beta_{\rm r}\, c$; here, $\beta_{\rm r} = 0.05$
- Surface temperature of blobs $T_{\rm blob} = T_{\rm disk}(r_{\rm tr})\,(r/r_{\rm tr})^{-p}$

Investigate the effect of different radial blob-temperature profiles (varying p)

Light curves:

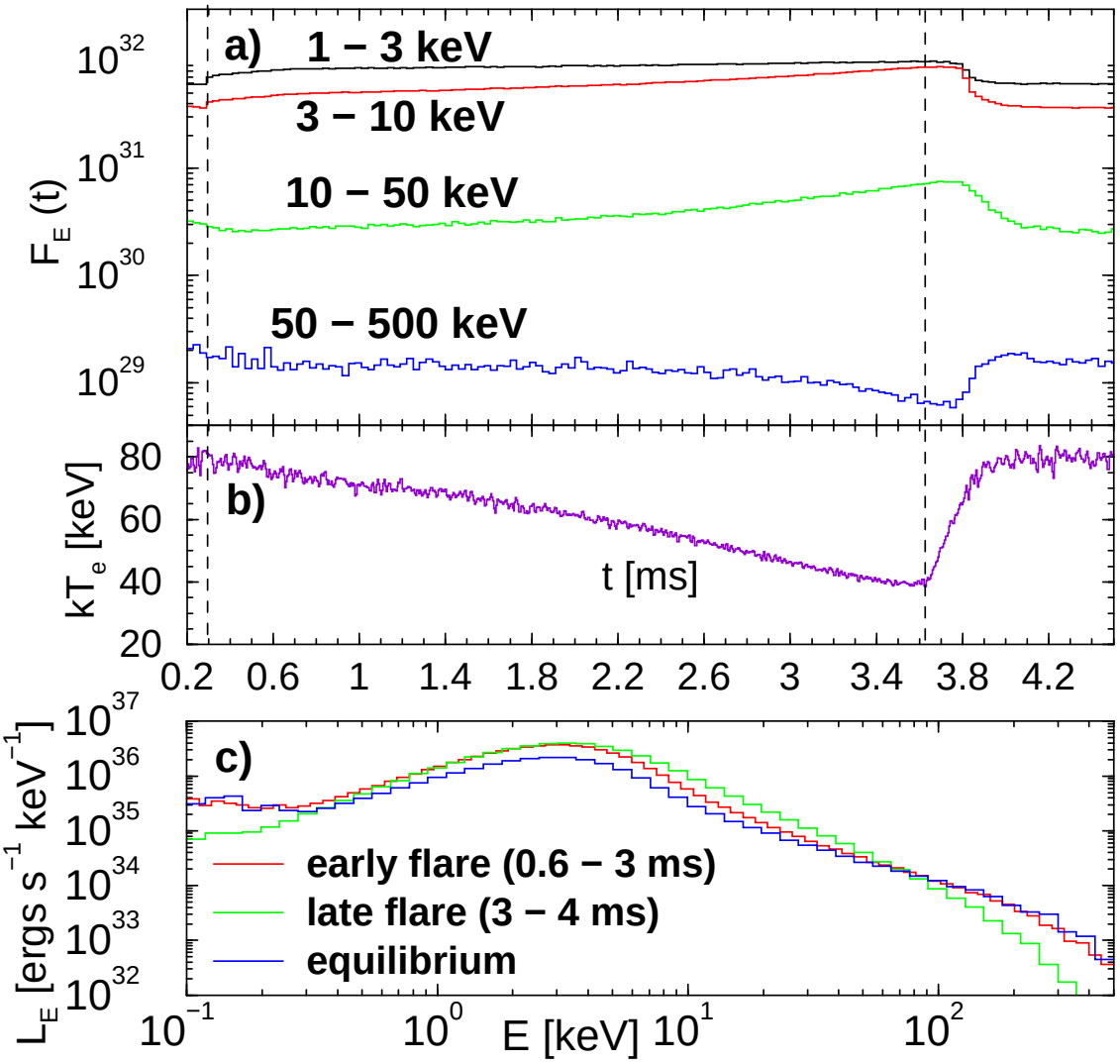

Fig. 8: *Energy-dependent light curves (a), evolution of the average coronal temperature (b), and snap-shot spectra (c) resulting from the inward-drifting blob scenario with* $T_{\rm blob} \propto r^{-0.25}$

Phase and time lags:

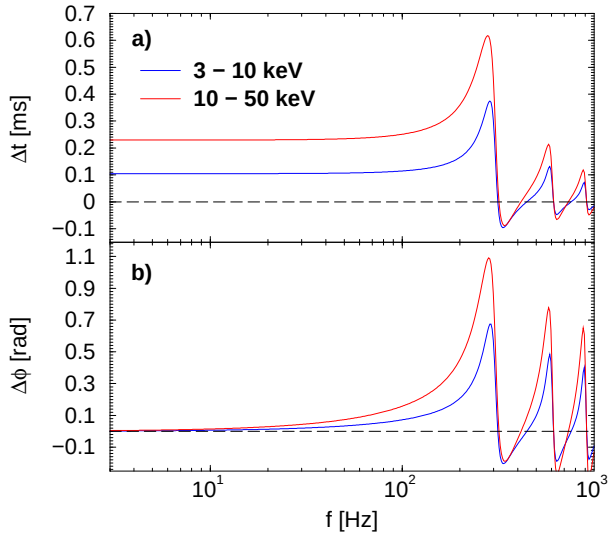

Fig. 9: *Time (a) and phase (b) lags w.r.t. the 1 – 3 keV channel, resulting from the inward-drifting blob model assuming the same parameters as for Fig. 8*

Results for inward-drifting blob case

- Low- and high-energy flares up to $\lesssim 50$ keV
- Rms variability amplitude decreasing with increasing photon energy
- Power spectra become harder with increasing photon energy
- No linear time-lag vs. Fourier period relation
- Phase and time lags oscillating between subsequent harmonics of fundamental frequency at $f_0 \sim r_{\rm tr}/(\beta_{\rm r} c)$. — Assuming slower drift velocities, this could be related to the alternating phase lags seen in GRS 1915+105 (Cui 1999, Reig et al. 2000, Lin et al. 2000) and in XTE J1550-564 (Wijnands, Homan & van der Klis 1999, Cui, Zhang & Chen 2000).

References

Bisnovatyi-Kogan, G. S., & Blinnikov, S. I., 1977, A&A, 59, 111

Blandford, R. D., & Begelman, M. C., 1999, MNRAS, 303, L1

Böttcher, M., & Liang, E. P., 1998, ApJ, 506, 281

Böttcher, M., & Liang, E. P., 1999, ApJ, 511, L37

Böttcher, M., & Liang, E. P., 2001, ApJ, 551, in press

Chen, X., et al., 1995, ApJ, 443, L61

Cui, W., 1999, ApJ, 524, L59

Cui, W., Zhang, S. N., & Chen, W., 2000, ApJ, 531, L45

Esin, A. A., et al., 1998, ApJ, 505, 854

Hua, X.-M., Kazanas, D. & Titarchuk, L., 1997, ApJ, 428, L57

Kazanas, D., Hua, X.-M. & Titarchuk, L. 1997, ApJ, 480, 735

Liang, E. P., & Price, R. H., 1977, ApJ, 218, 427

Lin, D., et al., 2000, ApJ, 531, 963

Maccarone, T. J., Coppi, P. S., & Poutanen, J., 2000, ApJ, 537, L107

Malzac, J., & Jourdain, E., 2000, A&A, 359, 843

Narayan, R., McClintock, J. E., & Yi, I., 1996, ApJ, 457, 821

Paul, B., et al., 1998a, A&AS, 128, 145

Paul, B., et al., 1998b, ApJ, 492, L63

Quataert, E., & Gruzinov, A., 2000, ApJ, 539, 809

Reig, P., et al., 2000, ApJ, 541, 883

Shakura, N. I., & Sunyaev, R. A., 1973, A&A, 24, 337

Wijnands, R., Homan, J., & van der Klis, M., 1999, ApJ, 526, L33